BBA - Molecular Cell Research 1865 (2018) 1640–1648

Contents lists available at ScienceDirect

BBA - Molecular Cell Research

journal homepage: www.elsevier.com/locate/bbamcr

Profiling of signal sequence characteristics and requirement of different translocation components

Chewon Yim[1], Sung-jun Jung[1], Ji Eun Hani Kim, Yunjae Jung, Seoyoon Dymphna Jeong, Hyun Kim*

School of Biological Sciences, Seoul National University, Seoul 08826, South Korea

ARTICLE INFO

Keywords:
Signal sequence
Endoplasmic reticulum
Protein translocation
Sec62
Yeast
Sec71

ABSTRACT

The N-terminal signal sequence (SS) on proteins targeted to the endoplasmic reticulum (ER) is surprisingly diverse in hydrophobicity, in the number of preceding N-terminal residues (N-length), and in charged residues flanking the sequence. However, it remains unclear how these sequences despite their heterogeneity bind to the same site and open the Sec61 translocon. We assessed varying features of SSs and their efficiencies in initiating translocation across the ER by using 5-min radiolabeling in yeast. We found that while hydrophobic SSs with a short N-length efficiently initiated translocation in Sec62 mutant, Sec63 mutant and Sec72 deletion strains, most SSs showed varying degrees of translocation defect in these strains. In particular, Sec71 was required for internal hydrophobic SSs to efficiently initiate translocation. These results suggest that different combinations of Sec62, Sec63, Sec71 and Sec72 dynamically associate with the Sec61 translocon for the optimal binding of incoming SSs of broad characteristics and the initiation of protein translocation *in vivo*.

1. Introduction

In eukaryotes, approximately 30% of proteins enter the endoplasmic reticulum (ER), and their entry into the ER begins the process of protein trafficking along the secretory pathway. A prerequisite to enter this pathway is the presence of a signal sequence (SS) [1]. Generally it is said that N-terminally positioned SSs or so-called signal peptides (SPs) are cleaved by signal peptidase, whereas more internally located SSs, conventionally referred to as signal-anchored (SA) sequences, are not cleaved by signal peptidase. However, SPs and SAs harbor similar sequence contexts and the presence of a signal peptidase cleavage site is not the sole determinant for whether an SS is cleaved or not [2], which makes it difficult to distinguish SPs and SAs. When a hydrophobic SS of a nascent chain emerges from the ribosome exit tunnel, it is recognized by the signal recognition particle (SRP) and guided to the ER membrane [3–5]. Less hydrophobic SSs are not recognized by SRP but are targeted to the ER by cytosolic chaperones that bind the mature part of the nascent chain [6–8]. After reaching the ER, SSs initiate protein translocation through the Sec61/α/Y translocon, a main pore-forming channel in the ER membrane [9–17].

Recently, the SRP-independent targeting (SND) pathway has been suggested to target and translocate proteins containing a transmembrane domain (TMD) located in the middle of the protein or toward the C-terminus of the protein, whereas the guided entry of tail-anchored proteins (GET) pathway serves to translocate proteins harboring a C-terminal tail-anchored sequence [18–20].

SSs consist of three parts: the hydrophobic core (H) and the flanking N- and C-terminal regions. While the basic structure of SSs is relatively simple, great diversity lies in the length and hydrophobicity of the H-region and the length and the charge distribution of the N- and C-terminal flanking regions [21–23]. Numerous studies have revealed that these features influence the orientation of SSs at the Sec translocon [24–35]. However, how various types of SSs bind to the Sec translocon and open the channel for protein translocation is poorly defined.

The Sec62/63 complex is composed of Sec62, Sec63, Sec71 and Sec72 and associates with the Sec61 channel for post-translational translocation [36–38]. However, Sec62 and Sec63 are also shown to mediate SRP-dependent and co-translational translocation of SA and membrane proteins [39–43]. Further, mammalian homologs of Sec62 and Sec63 are found to be associated with ribosomes [44]. Beyond the role in post-translational translocation, these studies implicate an expanded function of the Sec62/63 complex in co-translational translocation. A proximity-specific ribosome profiling study suggests that neither SRP dependence nor independence confer a strict preference of

* Corresponding author at: School of Biological Sciences, Building 504-421, Seoul National University, Seoul 08826, South Korea.
E-mail address: joy@snu.ac.kr (H. Kim).
[1] These authors contributed equally.

https://doi.org/10.1016/j.bbamcr.2018.08.018
Received 27 June 2018; Received in revised form 23 August 2018; Accepted 27 August 2018
Available online 29 August 2018
0167-4889/ © 2018 Elsevier B.V. All rights reserved.

proteins to co- or post-translational translocation [45]. Thus, increasing evidence points to a more intricate interplay between SSs, SRP, and the Sec62/63 complex than is previously thought, and we undertook to investigate their relationships in the context of varying features of SSs.

First, we assessed the heterogeneity of SSs in terms of their hydrophobicity and the length of the N-terminus preceding the SS (N-length) and determined how these characteristics affect SS efficiency. Our data show that increasing N-length impaired the function of moderately hydrophobic SSs but not that of highly hydrophobic SSs, indicating that short N-length is an important feature for moderately hydrophobic SSs. Our analysis of natural proteins shows that moderately hydrophobic SSs indeed have a shorter N-length than hydrophobic SSs. Next, we assessed how the diversity in SSs function in SRP, Sec62, Sec63, Sec71 and Sec72 defective yeast strains by metabolic labeling. We found that moderately hydrophobic SSs with a short N-length required all four components of the Sec62/63 complex for efficient translocation initiation whereas more hydrophobic SSs with the same N-length were independent of Sec62, Sec63 and Sec72, indicating that the latter are more translocation efficient SSs. Surprisingly, Sec71 was critical for efficient translocation initiation of hydrophobic SSs, especially internal ones. Overexpression of Sec62, Sec63 or Sec72 in *sec71*Δ did not complement translocation defects of Sec71-dependent substrates, implying a distinctive role of Sec71 in sorting internal hydrophobic SSs. These results suggest that different targeting and translocation components decode and sort signal sequence characteristics for proper initiation of protein translocation *in vivo*.

2. Materials and methods

2.1. Yeast strains

The *Saccharomyces cerevisiae* haploid W303-1α (*MATα*, *ade2*, *can1*, *his3*, *leu2*, *trp1*, *ura3*) was used as WT strain [46]. Construction of the *sec62 35DDD* mutant strain (*MATα*, *sec62Δ::HIS3*, *ade2*, *can1*, *his3*, *leu2*, *trp1*, *ura3, p415 1 kb upstream + sec62 35DDD*) was described in [39]. *sec63 A179T* strain was generated as follows. W303-1α was transformed with pRS416 1 kb upstream + *SEC63*. Genomic *SEC63* copy was deleted by homologous recombination of transformed *HIS3* cassette amplified from pCgH [47]. The resultant cells were transformed with pRS415 1 kb upstream + *sec63 A179T*. pRS416 1 kb upstream + *SEC63* was removed by FOA selection. The genomic ORF of *SEC71* or *SEC72* in W303-1α were substituted by *HIS3* marker amplified from pCgH vector by homologous recombination, and *sec71*Δ (*MATα*, *sec71Δ::HIS3*, *ade2*, *can1*, *his3*, *leu2*, *trp1*, *ura3*) and *sec72*Δ (*MATα*, *sec72Δ::HIS3*, *ade2*, *can1*, *his3*, *leu2*, *trp1*, *ura3*) strains were generated. For overexpression of Sec components, pRS425GPD overexpression vector carrying *SEC62-FLAG*, *SEC63-FLAG*, *SEC72-FLAG*, or *SEC71-3XHA* was transformed into either the *sec71Δ* strain or the genomic Sec71 HA-tagged strain (*MATα*, *sec63Δ::HIS3*, *sec71::HA-G418 ade2*, *can1*, *his3*, *leu2*, *trp1*, *ura3*, pURA-SEC63). For endogenous expression in *sec71Δ* strain, pRS415 1 kb upstream + *SEC62-FLAG*, *SEC63-FLAG* or *SEC72-FLAG* was transformed into the *sec71*Δ strain.

2.2. Construction of plasmids

To generate a vector encoding CPY, a pair of oligonucleotide primers containing 30 bases complementing the upstream and downstream sequences of the *SmaI* site in pRS424GPDHA vector [40] and annealing sequences for 5′ and 3′ end of the *PRC1* (*CPY*) gene were synthesized. The *PRC1* (*CPY*) ORF was amplified from genomic DNA of W303-1α by using these primers, and the resulting PCR products were transformed into W303-1α with a *SmaI* digested pRS424GPDHA vector for homologous recombination as described in [48]. Using the resultant plasmid (pRS424GPD*CPYHA*) as template, a *SmaI* site was introduced between the 2nd and 3rd residues of *CPY* by site-directed mutagenesis following manufacture's protocols (Toyobo, Japan). The N-terminal sequences of Dap2 and Sec71 were amplified from genomic DNA and inserted into a *SmaI* digested pRS424GPD*CPYHA* vector to generate pRS424GPD*D27CPY(1.9)HA* and pRS424GPD*S30CPY(1.5)HA* vectors, respectively. All other CPY variant plasmids were created by site-directed mutagenesis from these two vectors. To construct overexpression vectors containing *SEC62*, *SEC63* or *SEC72*, the corresponding ORFs were cloned under a GPD promoter in pRS425 plasmid by homologous recombination or using the Gibson assembly kit following the manufacture's protocol. *FLAG* tag was introduced by site-directed mutagenesis. Sec71 was cloned into pRS425GPDHA vector by homologous recombination.

2.3. Western blot analysis

To check overexpression of Sec components, 1.6 OD_{600} unit cells overexpressing each Sec component and a model protein were harvested after an overnight incubation at 30 °C. Cells were mixed with 60 μl of SDS sample buffer (50 mM Tris-HCl, pH 7.5, 5% SDS, 5% glycerol, 50 mM EDTA, pH 8, 50 mM DTT, 1 × protease inhibitor cocktail (Quartett, Germany, PPI1015), 1 mM PMSF) and boiled at 95 °C for 5 min. Samples were subjected to SDS-PAGE and Western blotting.

2.4. Pulse-labeling and immunoprecipitation

For W303-1α, *sec62 35DDD, sec71*Δ and *sec72*Δ strains, protein radiolabeling with [^{35}S]Met and immunoprecipitation were carried out as described in [40]. For *sec63 A179T*, cells were starved for 15 min at a non-permissive temperature (37 °C). For *sec65-1*, cells were shifted to 37 °C for an additional 30 min incubation prior to the 15min starvation at 37 °C. Immunoprecipitated proteins were prepared with 60 μl of sample buffer, subjected to SDS-PAGE and autoradiography, visualized with Typhoon™ FLA 7000, and then quantified with the Multi-GaugeV3.0 software.

2.5. Tunicamycin treatment

Prior to radiolabeling with [^{35}S]Met, 1.5 OD_{600} unit cells per reaction were harvested and pre-incubated in 1 ml of –Met synthetic defined medium with tunicamycin (Sigma, 100 μg·ml) for 15 min at 30 °C. After pre-incubation, cells were pelleted down and resuspended in 150 μl of –Met synthetic defined medium containing tunicamycin to maintain the same concentration throughout radiolabeling time.

2.6. Carbonate extraction

5–10 OD_{600} units of cells were grown overnight and harvested. Cells were resuspended in 200 μl of lysis buffer (20 mM Tris-HCl, pH 8.0, 10 mM EDTA, pH 8.0, 100 mM NaCl, 300 mM sorbitol, 1 mM PMSF, 1 × protease inhibitor) and vortexed with glass beads for 10 min at 4 °C. The lysate was transferred to a new pre-chilled tube after a quick spin down. The remaining glass beads were washed with 200 μl of lysis buffer, the lysate of which was added to the final lysate. Unbroken cells were removed by centrifugation for 30 s at 14,000 RPM on a desk-top centrifuge and the lysate was transferred to two pre-chilled tubes, one for the 'total' fraction and the other for carbonate extraction. For carbonate extraction, 300 μl of 0.1 M Na_2CO_3 (pH 11.5) was added to the lysate, and the reaction was incubated for 30 min on ice prior to centrifugation for 20 min at 14,000 RPM. The resulting supernatant was saved as the 'supernatant' fraction in another E-tube, and the pellet was resuspended and washed with 200 μl of Na_2CO_3 and centrifuged for 20 min at 14,000 RPM. After removal of Na_2CO_3 solution from the pellet, 'total', 'supernatant' and 'pellet' fractions were incubated with TCA (final concentration 12.5%) for 30 min on ice. Precipitated proteins were washed with 100% acetone, saved for sample preparation with 60 μl of sample buffer and analyzed by SDS-PAGE and Western blotting.

2.7. Prediction of N-length and ΔG_{app} value of SS

N-length and ΔG_{app} value of SSs of all proteins were calculated on the ΔG prediction server v1.0 (http://dgpred.cbr.su.se/). After submission of full protein sequence of each protein to "full protein scan", the ΔG_{app} value was obtained and the number of N-terminal amino acids before the first predicted TMD was counted. Each CPY variant is named following the nomenclature D/S/A(N-length)CPY(ΔG_{app}), indicating N-length and ΔG_{app} value.

2.8. Bioinformatics analysis of yeast SP and SA proteins

The sequence information of yeast SP and SA proteins were extracted from the UniProtKB Protein Knowledgebase by querying "signal peptide" or "signal anchor", respectively, and "*Saccharomyces cerevisiae*". The downloaded data set was combined with the list containing SPs and SAs in [40]. Protein sequences of the combined list were run on the ΔG prediction program (http://dgpred.cbr.su.se) [49], and the position, amino acid sequences and the ΔG_{app} values of SSs were collected. Proteins predicted to localize to other organelles, to have more than two TMDs [50], or not to have predicted SSs within the first 60 amino acids were manually sorted.

2.9. Statistical analysis

All statistical analysis was performed using Microsoft Excel 2013 for Windows. All graph and box plots were created using this program.

3. Results

3.1. Translocation of CPY is sensitive to N-length

To evaluate the relationship between the number of residues preceding the SS (that is, N-length) and translocation efficiency, we prepared a set of test proteins from a well-characterized secretory protein carboxypeptidase Y (CPY, YMR297W), which contains a moderately hydrophobic SS [51–53]. Two extensions, each derived from N-terminal residues of single-spanning ER membrane proteins, Dap2 (YHR028C) and Sec71 (YBR171W), were fused to the N-terminus of CPY and gradually truncated (D CPYs and S CPYs) (Fig. 1A and Table 1). Dap2 and Sec71 form opposite membrane topologies; the former orients as N_{cyto}-C_{lumen} (type II) and the latter as N_{lumen}-C_{cyto} (type I). Since their N-terminal ends are naturally oriented to the cytosol and lumen, respectively, possible residue-specific effects on translocation could be monitored (Table 1). Notably, the predicted length and hydrophobicity of SSs slightly varied depending on overall sequence context.

Translocation efficiencies of these constructs were assessed by radiolabeling with [^{35}S]Met for 5 min at 30 °C, capturing the initial translocation status *in vivo* (Fig. 1B). Translocation of CPY chimeras was judged by N-linked glycosylation which occurs only when the C-terminal domain of CPY is translocated into the ER lumen, resulting in a size upshift on SDS-PAGE. Glycosylation efficiencies of CPY constructs were plotted against N-length (Fig. 1D). Glycosylated products were detected with N-length extensions < 12 residues for both sets, indicating that translocation of CPY was inhibited by longer N-length extensions regardless of their original orientations or sequence compositions (Fig. 1B). In other words, the N-length overrode the effects of possible contributions of individual or overall sequence composition within the N-length. These results suggest that long extensions at the N-terminus of CPY inhibits translocation.

3.2. Translocation of CPY with long N-length is sensitive to hydrophobicity of SSs

Next, keeping the longest N-length, the hydrophobicity of the SS in D27CPY(1.9) and S30CPY(1.5) was systematically increased by mutagenesis (D27CPY(ΔG_{app}) and S30CPY(ΔG_{app})) (Fig. 1A and Table 1). The SS position and hydrophobicity were calculated with the ΔG predictor. The apparent free energy for membrane insertion (ΔG_{app}) describes how favorable or unfavorable a segment is to be inserted into the membrane *via* the Sec61 translocon. Since protein translocation into the ER is initiated by binding of an SS at the Sec61 translocon, we reasoned that hydrophobicity estimation by ΔG predictor would be most appropriate as a proxy for membrane insertion (Table 1).

WT cells bearing the model proteins were radiolabeled for 5 min at 30 °C (Fig. 1C). We observed > 50% translocation when the ΔG_{app} value of the SS was lower than −1.0 kcal/mol for D CPY(ΔG_{app}) variants (Fig. 1C, *left*). Restoration of translocation was observed for S CPY (ΔG_{app}) variants when ΔG_{app} value dropped to 0.5 kcal/mol or lower (Fig. 1C, *right*). A negative correlation between glycosylation efficiency and ΔG_{app} values for CPY variants with a long N-length (Fig. 1E), indicating that translocation defects due to a long N-length could be overcome by increased hydrophobicity of SSs.

Because internal SSs are often membrane anchored, we assessed whether increasing hydrophobicity can convert a SS to a SA sequence. To better distinguish SS-cleaved, glycosylated CPY from uncleaved glycosylated form, cells were treated with tunicamycin (Tm) to block *in vivo* N-linked glycosylation (Fig. 1C). Upon Tm treatment, two bands were observed: one that migrated to the same size as the untargeted, full-length form and another band, denoting the SS-cleaved form, that migrated faster. D22CPY(-2.6) generated a full-length glycosylated product, indicating that its SS remains uncleaved. By carbonate extraction, it was confirmed that this construct becomes membrane-anchored (Fig. S1). Because the N-length, the SS cleavage site and the mature part of CPY were the same for all D CPY(ΔG_{app}) chimeras, which differed only in terms of the hydrophobicity of SS, the observed differences in cleavage efficiency can be solely attributable to SS hydrophobicity. It was previously observed that hydrophilic SSs were cleaved by signal peptidase whereas hydrophobic ones in the same protein context were not, resulting in a membrane-anchored protein [54]. These results show that SSs with a longer N-length require a highly hydrophobic core sequence and can be membrane anchored.

3.3. Correlation between the hydrophobicity of SSs and their N-length

To further investigate the relationship between N-length and hydrophobicity of SSs, we additionally prepared constructs that contain SSs of intermediate hydrophobicity and N-length (D18CPY(0.1) and D18CPY(-1.0)). For possible effects of the extended N-terminal residues in D CPY and S CPY variants, two constructs that contain only Ala residues at the N-terminus were also prepared (A8CPY(0.5) and A13CPY (-0.5)), and translocation efficiencies of these constructs were assessed. Of all the tested model proteins, those that resulted in > 15% translocation at 5 min of *in vivo* radiolabeling were plotted (Fig. 1F). This cutoff value was set to illustrate the initial engagement of polypeptides to the translocon. We noticed that the ratio of translocated products further increased when assessed by pulse-chase or Western blotting, meaning that efficient initial engagement is a good indicator of a successful translocation. Thus, we used this value to define the threshold N-length at a given hydrophobicity. Our results show that moderately hydrophobic CPY SSs have shorter threshold N-length than sufficiently hydrophobic CPY SS variants (10 at $\Delta G_{app} = 1.9$ and 27 at $\Delta G_{app} = -1.0$ (kcal/mol)).

3.4. Distribution of N-length and hydrophobicity of SSs in natural proteins

To confirm whether our findings with the model constructs could be generalized, we determined the N-length and hydrophobicity of SSs in natural proteins. Proteins that are predicted to be part of the secretome or SignalP positive were selected from the list in [45]. We extracted a total of 854 proteins, excluding proteins that were predicted not to have SS or TMD within the first 60 residues (Table S1). To avoid possible

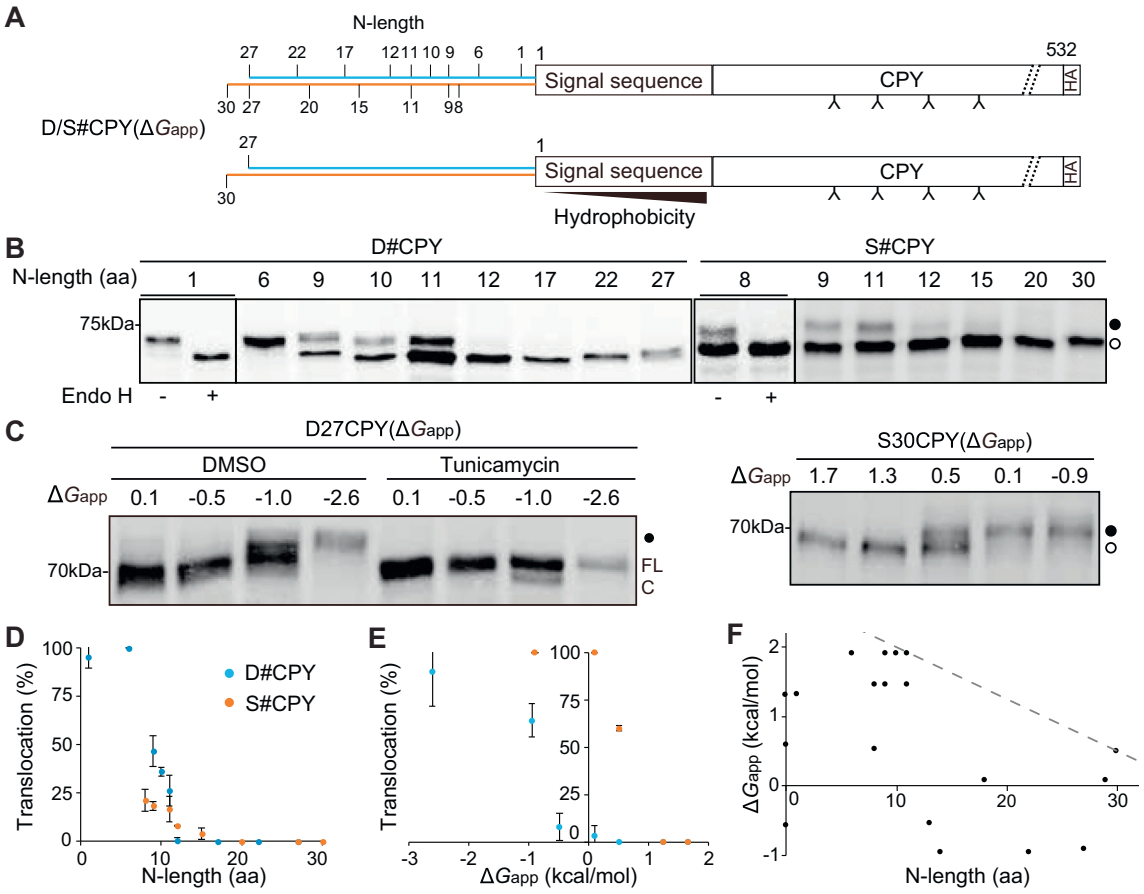

Fig. 1. N-length extensions reduce initial protein translocation efficiency of CPY into the ER. (A) Schematics of D/S#CPY(ΔG_{app}) length (*top*) and SS hydrophobicity (*bottom*) variants (D CPY, blue; S CPY, orange). N-length values of D#CPY and S#CPY are indicated. 'Y' indicates N-linked glycosylation sites. D/S#CPY(ΔG_{app}) variants were fused with three copies of HA epitope for immunoprecipitation. (B) W303-1α expressing indicated D#CPY (*left*) or S#CPY (*right*) was radiolabeled with S^{35}[MET] for 5 min. Radiolabeled D#CPY was immunoprecipitated using HA antibody, subjected to SDS-PAGE (7% gel) and visualized by autoradiography. D1CPY (1.3) and S8CPY(1.5) samples were incubated in the presence or the absence of endoglycosidase H (Endo H) prior to SDS-PAGE. Open and closed circles indicate glycosylated and non-glycosylated bands, respectively. aa, amino acids. (C) *Left*, W303-1α cells expressing D27CPY(ΔG_{app}) of indicated ΔG_{app} values were radiolabeled in the presence or the absence of Tunicamycin. Translocation assay was done as in Fig. 1B. FL, full length proteins. C, cleaved products. *Right*, S30CPY (ΔG_{app}) variants expressed in W303-1α were analyzed as in Fig. 1B. See also Fig. S1. (D) Quantified data of (B). Translocation efficiency ([Glycosylated band (%) / Total]) of D#CPY (blue) and S#CPY (orange) was plotted. (E) Quantified data of (C). The translocation efficiency of D27CPY(ΔG_{app}) and S30CPY(ΔG_{app}) was plotted. (F) CPY variants (listed in Table 1) in W303-1α were analyzed as in (B). ΔG_{app} (kcal/mol) and N-length (amino acids) of CPY variants with > 15% translocation efficiency at 5 min radiolabeling were plotted.

effects of downstream TMD in targeting and translocation [55,56], proteins that were predicted to have more than two TMDs [50] were also excluded. The final set included 494 proteins containing a predicted single SS within the first 60 residues of the protein (Table S2). For each protein, the hydrophobicity of the SS or the TMD was calculated using the ΔG predictor. When the N-length and hydrophobicity of the SSs were plotted, we found that the majority of the proteins fell on the left side of the experimentally measured N-length threshold (Fig. 2A).

To determine the relationship between N-length and SS hydrophobicity of these natural proteins, hydrophobicity values were sorted in boxes with a 3-residue-window of N-length (Fig. 2B). For N-lengths shorter than 10–12 residues, a negative correlation between N-length and SS hydrophobicity was observed: the shorter the N-length, the higher the ΔG_{app} or the lower the hydrophobicity. An N-length of 10–12 residues is in good agreement with the experimentally measured N-length threshold for CPY (11 residues), the hydrophobicity of which is 1.9 kcal/mol (Fig. 1B and D). For proteins with N-length longer than 12 residues, there was no significant correlation between N-length and hydrophobicity of SSs.

Next, the distribution of N-length in a given ΔG_{app} range of hydrophobicity was sorted (Fig. 2C). We found that proteins with SS hydrophobicity lower than a ΔG_{app} value of −0.5 kcal/mol tend to have a broader range of N-length, indicating that they are insensitive to N-length. For the less hydrophobic SSs (ΔG_{app} > 0.5 kcal/mol), the overall N-length is much shorter than that of highly hydrophobic SSs (ΔG_{app} < −1.5 kcal/mol). When the dataset included multi-spanning membrane proteins, the same pattern between N-length and SS hydrophobicity was still observed (Fig. S2). Our analysis with natural proteins confirms that hydrophilic SSs tend to have a shorter N-length and that the N-length is less critical for hydrophobic SSs.

3.5. SSs of varying characteristics require different sets of targeting and translocation components

To determine whether and which targeting and Sec components are required for the different types of SSs, we assessed translocation efficiencies of CPY variants in strains either defective or depleted of one of components of the Sec62/63 complex (*sec62 35DDD*, *sec63 A179T*, *sec71*Δ and *sec72*Δ) or SRP (*sec65-1*). The Sec62/63 complex comprises of Sec62, Sec63, Sec71 and Sec72 [36,57]. For Sec62 and Sec63, we used mutant strains. *sec62 35DDD* mutant carries three substituted Asp residues in the N-terminus, and the mutation impairs interaction of Sec62 with Sec63 [39]. *sec63 A179T* was prepared by site-directed

Table 1
List of CPY variants and natural proteins used in this study. CPY variants used in this study are listed. N-length indicates the number of amino acids preceding the SS of CPY whose sequences and ΔG_{app} (kcal/mol) values are also shown. Predicted SS is underlined and mutations within the CPY SS are marked in bold.

Name	N-terminal sequence	ΔG_{app} [a]	N-length
CPY	MKAFTSLLCGLGLSTTLAKAISL	1.299	0
D27CPY(1.9)	MEGGEEEVERIPDELFDTKKKHLLDKKAF**S**SLLCGLGLSTTLAKAISL	1.921	27
D22CPY(1.9)	MEVERIPDELFDTKKKHLLDKKAF**S**SLLCGLGLSTTLAKAISL	1.921	22
D17CPY(1.9)	MPDELFDTKKKHLLDKKAF**S**SLLCGLGLSTTLAKAISL	1.921	17
D12CPY(1.9)	MDTKKKHLLDKKAF**S**SLLCGLGLSTTLAKAISL	1.921	12
D11CPY(1.9)	MTKKKHLLDKKAF**S**SLLCGLGLSTTLAKAISL	1.921	11
D10CPY(1.9)	MKKKHLLDKKAF**S**SLLCGLGLSTTLAKAISL	1.921	10
D9CPY(1.9)	MKKHLLDKKAF**S**SLLCGLGLSTTLAKAISL	1.921	9
D6CPY(1.9)	MLLDKKAF**S**SLLCGLGLSTTLAKAISL	1.921	6
D1CPY(1.3)	MLKAF**S**SLLCGLGLSTTLAKAISL	1.334	1
S30CPY(1.5)	MSEFNETKFSNNSTFFETEEPIVETKSISKAFTSLLCGLGLSTTLAKAISL	1.465	30
S27CPY(1.5)	MNETKFSNNSTFFETEEPIVETKSISKAFTSLLCGLGLSTTLAKAISL	1.465	27
S20CPY(1.5)	MNSTFFETEEPIVETKSISKAFTSLLCGLGLSTTLAKAISL	1.465	20
S15CPY(1.5)	METEEPIVETKSISKAFTSLLCGLGLSTTLAKAISL	1.465	15
S12CPY(1.5)	MEPIVETKSISKAFTSLLCGLGLSTTLAKAISL	1.465	12
S11CPY(1.5)	MPIVETKSISKAFTSLLCGLGLSTTLAKAISL	1.465	11
S9CPY(1.5)	MPIVESISKAFTSLLCGLGLSTTLAKAISL	1.465	9
S8CPY(1.5)	METKSISKAFTSLLCGLGLSTTLAKAISL	1.465	8
A8CPY(0.5)	MAAAAAAAAAAKAFTSLL**C**LLGLSTTLAKAI	0.546	8
A13CPY(0.5)	MAAAAAAAAAAAAAAAKAFTSLL**C**LLGLSTTLAKAI	0.546	13
A13CPY(-0.5)	MAAAAAAAAAAAAAAAKAFTSLL**C**LLLLSTTLAKAI	−0.526	13
D18CPY(0.1)	MRIPDELFDTKKKHLLDKKAF**S**SLL**C**LLLLSTTLAKAISL	0.098	18
D18CPY(-1.0)	MRIPDELFDTKKKHLLDK**L**AF**S**SLL**C**LLLLSTTLA	−0.95	14
D27CPY(1.7)	MEGGEEEVERIPDELFDTKKKHLLDKKAF**S**SLL**C**ALGLSTTLAKAISL	1.656	27
D26CPY(1.3)	MEGGEEEVERIPDELFDTKKKHLLDKKAF**S**SLL**C**LLGLSTTLAKAISL	1.253	26
D27CPY(0.5)	MEGGEEEVERIPDELFDTKKKHLLDKKAF**S**SLL**C**ALLLSTTLAKAISL	0.506	27
D26CPY(0.1)	MEGGEEEVERIPDELFDTKKKHLLDKKAF**S**SLL**C**LLLLSTTLAKAISL	0.098	26
D22CPY(-0.5)	MEGGEEEVERIPDELFDTKKKHLLDKLAF**S**SLL**C**ALLLSTTLA	−0.487	22
D22CPY(-1.0)	MEGGEEEVERIPDELFDTKKKHLLDK**L**AF**S**SLL**C**LLLLSTTLA	−0.95	22
D22CPY(-2.6)	MEGGEEEVERIPDELFDTKKKHLLDK**LLL**T**L**LL**C**LLLLSTTLA	−2.615	22
S30CPY(1.7)	MSEFNETKFSNNSTFFETEEPIVETKSISKAF**S**SLL**C**ALGLSTTLAKAISL	1.656	30
S29CPY(1.3)	MSEFNETKFSNNSTFFETEEPIVETKSISKAF**S**SLL**C**LLGLSTTLAKAISL	1.253	29
S30CPY(0.5)	MSEFNETKFSNNSTFFETEEPIVETKSISKAF**S**SLL**C**ALLLSTTLAKAISL	0.506	30
S29CPY(0.1)	MSEFNETKFSNNSTFFETEEPIVETKSISKAF**S**SLL**C**LLLLSTTLAKAISL	0.098	29
S27CPY(-0.9)	MSEFNETKFSNNSTFFETEEPIVETKSI**S**LAF**S**SLL**C**LLLLSTTLA	−0.901	27
CPY(-0.6)	MKAFTSLL**C**LLLSTTLAKAISL	−0.551	0
CPY(-1.9)	MKL**L**TLLL**C**LLLSTTLAKAI	−1.850	0
Spc3	MFSFVQRFQNVSNQAFSMGIVMVVFIMASSYYQLI	0.337	14
Dap2	MEGGEEEVERIPDELFDTKKKHLLDKLIRVGIILVLLIWGTVLLL	−2.932	25

[a] The ΔG_{app} and position of the SS in CPY variants were predicted by the ΔG predictor (http://dgpred.cbr.su.se/). Note that the ΔG predictor predicted the position of a hydrophobic segment slightly differently depending on the sequence context.

mutagenesis, whose point mutation in the luminal J-domain of Sec63 has been shown to disrupt its interaction with the ER-chaperone Kar2 [58]. For Sec71 and Sec72, deletion strains were prepared (*sec71*Δ and *sec72*Δ). Finally, the well-established *sec65-1* strain that exhibits a temperature-sensitive defect in SRP function was used [46]. For simplicity, SSs of model proteins are indicated according to their N-length and hydrophobicity regardless of their origins; *e.g.* D/S/A#CPY(ΔG_{app}) as N#CPY(ΔG_{app}).

CPY(-0.6) and CPY(-1.9), two representative model proteins carrying a hydrophobic SS with no N-length extension were expressed in *sec62 35DDD*, *sec63 A179T*, *sec71*Δ, *sec72*Δ and *sec65-1* strains (Fig. 3A). The proteins were efficiently translocated in *sec62 35DDD*, *sec63 A179T* and *sec72*Δ cells whereas their translocation efficiency decreased in *sec71*Δ and *sec65-1* cells by ~25% and ~35% for CPY (-0.6) and CPY(-1.9), respectively.

Next, N1CPY(1.3) and N6CPY(1.9) variants that contain low hydrophobic SSs with a short N-length were tested. We found that the translocation of both CPY variants was significantly reduced in all mutant strains but *sec65-1*, showing an especially impaired defect in the *sec62 35DDD* strain (~80%P reduction compared to WT) (Fig. 3B).

We next assessed the translocation of N22CPY(-1.0) and N22CPY (-2.6) variants with an opposite SS profile to N1CPY(1.3) and N6CPY (1.9) variants (a hydrophobic SS with a long N-length as opposed to a hydrophilic SS with a shot N-length). Compared to WT, the translocation efficiency of N22CPY(-1.0) was ~50–70% reduced in *sec62 35DDD* and *sec72Δ* strains whereas the translocation efficiency of the more hydrophobic variant, N22CPY(-2.6), was unchanged, indicating that Sec62 and Sec72 sort less hydrophobic variants (Fig. 3C). For both variants, an approximately 30% reduction in translocation efficiency was observed in *sec63 A179T* cells. Meanwhile, translocation of both CPY variants was severely defective in *sec71*Δ and *sec65-1* strains, suggesting that such SSs are highly dependent on Sec71 and SRP function.

Lastly, CPY variants carrying SSs of intermediate hydrophobicity and N-length, N18CPY(0.1) and N18CPY(-1.0) were analyzed (Fig. 3D). Translocation of both variants were defective in all five mutant strains to different degrees. For the N18CPY(-1.0) variant, the translocation efficiency was ~40%P reduced in *sec62 35DDD*, *sec63 A179T* and *sec72*Δ strains whereas severe defects in translocation was observed in *sec71*Δ and *sec65-1* strains (90% and 70% reduction, respectively) (Fig. 3D). These results suggest that SRP and Sec components collaborate to guide SSs carrying intermediate hydrophobicity and N-length for proper binding to the Sec translocon and initiation of protein translocation through the ER.

In summary, Sec62/72 and SRP exhibited different SS specificities; Sec62/72 handles SSs of low hydrophobicity whereas SRP handles SSs of high hydrophobicity, in the CPY context. Consistent to a recent study, hydrophobic SSs were dependent on SRP regardless of N-length [8]. However, we noticed that the translocation of hydrophobic SSs with longer N-length was more defective than their counterparts with

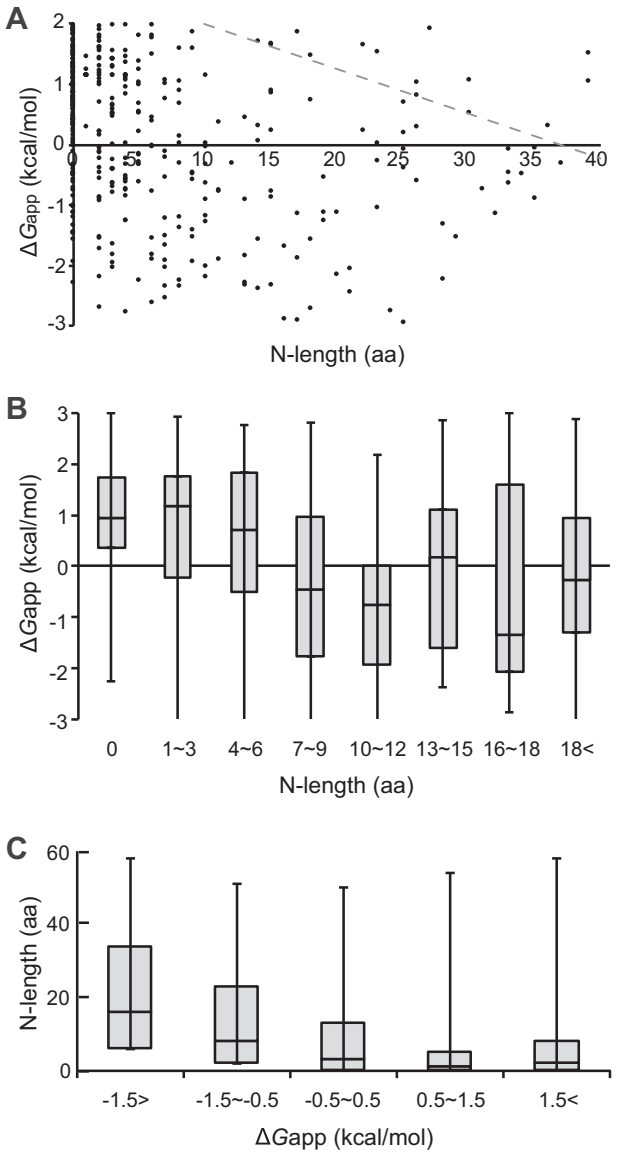

Fig. 2. Distribution of N-length and hydrophobicity of signal sequences in yeast proteins. See also Fig. S2. (A) Predicted ΔG_{app} values (kcal/mol) of SSs and N-length values (amino acids) of total 494 natural SP and SA proteins (listed in Table S2) in *Saccharomyces cerevisiae* were plotted. (B and C) The same set of proteins in (A) are sorted. Boxes and whiskers show 25–75 percentile values with min/max; the median is the central line in each box. (B) Distribution of ΔG_{app} (kcal/mol) of SSs in indicated ranges of N-length. (C) Distribution of N-length (amino acids) in indicated ranges of ΔG_{app} (kcal/mol).

shorter N-length in the *sec65-1* strain. Translocation of CPY variants for all types of SSs was defective in *sec71*Δ cells, and hydrophobic SSs with longer N-length was most defective, suggesting that Sec71 is essential for efficient translocation initiation *in vivo* and that its role is especially critical for internal hydrophobic SSs.

3.6. Natural proteins carrying SSs of varying hydrophobicity and N-length

To validate our results, we selected three natural proteins, Dap2, Spc3 (YLR066W) and CPY that contain SSs of varying N-length and hydrophobicity and assessed their translocation efficiencies in the same set of mutant strains (Fig. 3E). CPY contains an N-terminal cleavable SS with a G_{app} value of 1.3 kcal/mol. Dap2 is an SA protein that contains a 26-residue N-terminal segment preceding the SA sequence, which has a ΔG_{app} value of −2.9 kcal/mol. Spc3 has an SA sequence with a ΔG_{app} value of 0.3 kcal/mol and an N-length of 14 residues. Because all three proteins localize their C-terminus to the luminal side of the ER, their translocation efficiency could be assessed by glycosylation.

CPY variants with a less hydrophobic SS and a shorter N-length showed greater translocation defects in all mutant strains except *sec65-1* (Fig. 3E, *top*). Conversely, translocation of Dap2, which has a highly hydrophobic SS and a long N-length, was dramatically compromised in *sec65-1* and mildly defective in *sec63 A179T* and *sec71*Δ (Fig. 3E, *middle*). In comparison, translocation of Spc3, which has a marginally hydrophobic SS with an intermediate N-length, was defective in all mutant strains except the *sec72*Δ strain (Fig. 3E, *bottom*). Sec62 and SRP showed opposite substrate specificity; translocation of Dap2 was unaffected in *sec62 35DDD* but severely diminished in *sec65-1* while translocation of CPY was affected in *sec62 35DD* but not in *sec65-1*. It has been reported that the SRP receptor displaces Sec62 from an interaction with Sec61 for SRP-dependent translocation, implying antagonistic roles for Sec62 and SRP [59]. Albeit to different extents, translocation of all three proteins was defective in *sec63 A179T* and *sec71*Δ strains, with a higher severity of defect in the latter; these findings are consistent to our earlier observations with model substrates.

3.7. Sec71 distinctively functions in translocation of proteins carrying internal hydrophobic SSs

While initial translocation was impaired in the *sec71*Δ strain across all SS types, it was most pronounced for internal hydrophobic SSs (Fig. 3C). Since Sec71 is in complex with Sec62, Sec63 and Sec72, we next asked whether deletion of Sec71 destabilized the complex. In such case, overexpression of other subunits in the complex could rescue the phenotypic defects in yeast. Thus, we examined whether overexpression of Sec62, Sec63 or Sec72 could compensate for the loss of Sec71 function in translocating proteins carrying an internal hydrophobic SS. For this, translocation efficiency of N22CPY(-1.0) and N22CPY(-2.6) was assessed in *sec71*Δ cells overexpressing Sec62, Sec63 or Sec72 (Fig. 4A). Overexpression of Sec62, Sec63 or Sec72 did not restore translocation defects of N22CPY(-1.0) and N22CPY(-2.6) in *sec71*Δ strain, indicating that the function of Sec71 cannot be replaced by Sec62, Sec63 or Sec72 in translocation of proteins with such SS types.

Next, we wondered whether Sec71 alone is sufficient for translocation of proteins with internal hydrophobic SSs. If so, more copies of Sec71 might improve Sec71-dependent translocation. N22CPY(-0.5) and N22CPY(-1.0), which were incompletely translocated in WT strain (Fig. 1D), were expressed in cells overexpressing Sec71. Translocation of neither N22CPY(-0.5) nor N22CPY(-1.0) was further enhanced with Sec71 overexpression (Fig. 4B), suggesting that Sec71 is critical but not sufficient alone. Of note, Sec71 is indispensable for cell growth at 37 °C. Its role in stabilizing hydrophobic internal SSs may be especially essential at a higher temperature.

4. Discussion

The sequence characteristics of N-terminal signal sequences (SSs) on secretory and membrane proteins targeted to the ER are surprisingly diverse. In particular, the hydrophobicity of the hydrophobic core and the length and composition of N- and C-terminal flanking regions are uniquely heterogeneous. SSs are often referred to as endoplasmic reticulum (ER) targeting sequences, yet some are not recognized by the signal recognition particle (SRP) and are targeted to the ER *via* cytosolic chaperones that bind to the mature part of a nascent chain in an SRP-SS interaction independent pathway. Irrespective of how nascent chains are targeted to the ER, a key function of SSs is to bind to and open the protein-conducting channel to initiate the translocation of proteins across the ER membrane. While TMs 2 and 7 of Sec61/α/Y have been shown as the SS binding site [14–16], how diverse SSs bind to the same

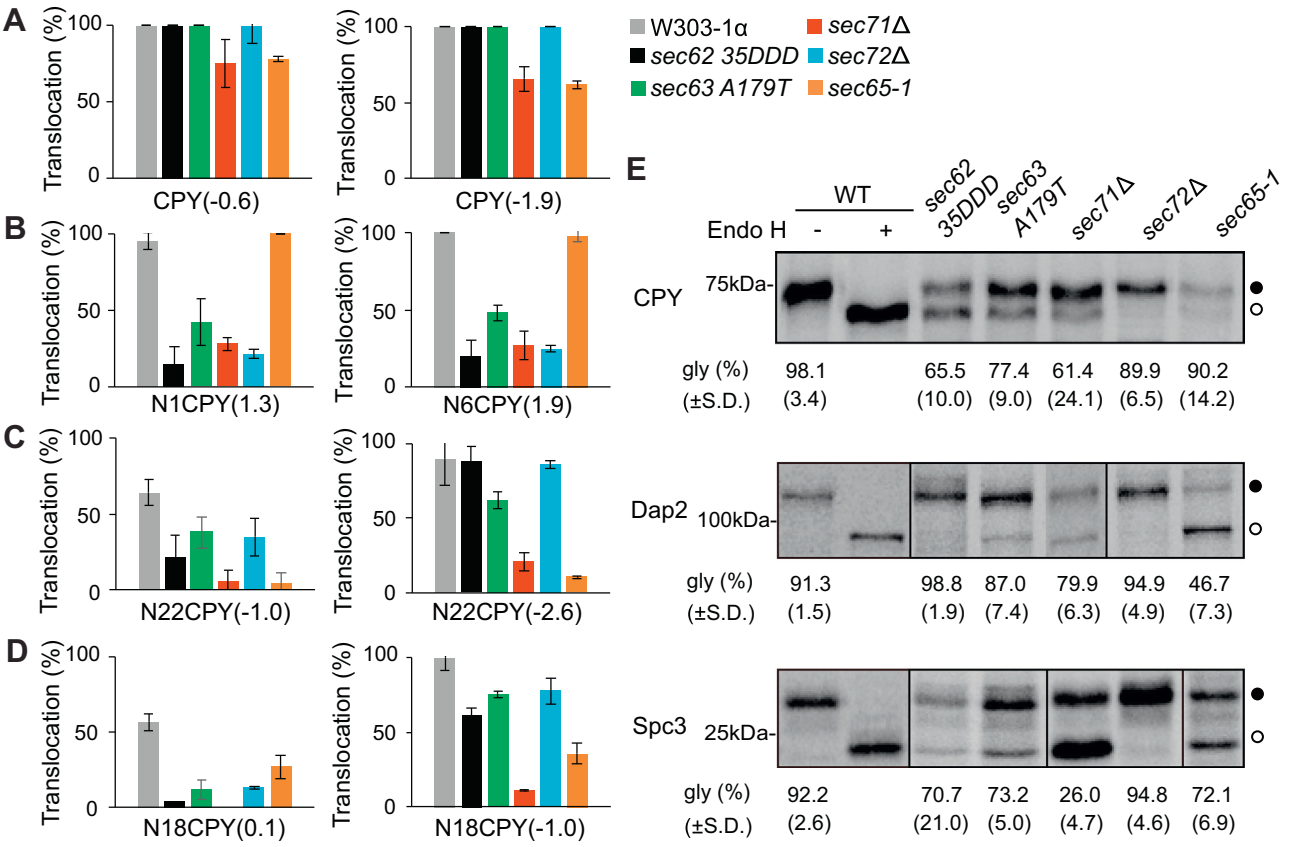

Fig. 3. Different combinations of Sec62/63 components and SRP are required for efficient translocation of proteins depending on signal sequence characteristics. (A to D) Indicated N#CPY(ΔG_{app}) variants (listed in Table 1), (E) yeast natural proteins in W303-1α and mutant strains were analyzed as done in Fig. 1B. For *sec65-1* and *sec63 A179T* temperature-sensitive mutant strains, growth/radiolabeling condition was modified as described in experimental procedures. The average translocation efficiency ([Glycosylated bands × 100 (%) / Total]) and standard deviation is indicated (n ≥ 3). 'N#', N-length (amino acids); predicted ΔG_{app} values (kcal/mol) of SSs in parentheses. (E) CPY (*top*), Dap2 (*middle*) and Spc3 (*bottom*) in W303-1α cell were treated with Endo H. The average translocation efficiency ([Glycosylated bands × 100 (%) / Total]) and standard deviation are indicated below (n = 3). Open and closed circles indicate glycosylated and non-glycosylated bands, respectively.

site and initiate translocation remain unknown.

We assessed the initial translocation efficiency of CPY variants carrying SSs systematically varied in N-length and hydrophobicity. Our results show that N-length should be < 10–12 residues for CPY SS to be efficient whereas CPY variants with a longer N-length required higher SS hydrophobicity. Further proteome-wide analyses of SS-containing yeast proteins also show a negative correlation between translocation efficiency and N-length in moderately hydrophobic SSs, implying that moderately hydrophobic SSs require a relatively shorter N-length to act as efficient SSs whereas highly hydrophobic SSs can have a broader range of N-lengths. Because we selected yeast proteins containing SSs or TMDs within the N-terminal 60 residues to assess targeting and translocation *via* SRP and/or the Sec62/63 complex, it means that for smaller proteins with a longer N-length the position of the TMD is shifted toward the C-terminus in comparison to larger proteins, and it is possible that they may be targeted by the GET pathway and/or the SND pathway [18–20,60].

It should be noted that the hydrophobicity of SSs was calculated with the ΔG predictor, which predicts the probability of a segment to be inserted into the membrane or not through the Sec61 translocon. A more positive ΔG_{app} value thus means that a SS would prefer to be in a more polar environment, while those of a more negative ΔG_{app}, a more nonpolar environment. Hydrophobic SSs with a short N-length did not require Sec62, Sec63, and Sec72; these findings suggest that they may be efficient SSs, to open the Sec61 translocon. However, SS that contains a longer N-length and/or less hydrophobic core region may be insufficient to open the Sec61 translocon on their own. Hence, these SSs may involve protein-protein interactions with Sec62/Sec63 components for proper binding and subsequent opening of the Sec61 channel. This idea is in line with recent studies in mammalian systems. By measuring SS efficiencies of Xbp1 arrested peptides through crosslinking, Kriegler et al. has shown that the way SSs engage the Sec translocon differ depending on the SS [61]. Moreover, Hassdenteufel et al. has shown that weak SSs require Sec62, Sec63 and Bip for successful ER translocation [62].

While Sec62/63/71/72 function together to ensure successful protein translocation initiated by moderately hydrophobic SSs with a short N-length, the translocation of internally located hydrophobic SSs was mostly dependent on Sec71 but not Sec62 and Sec72. Since the abundance of the four components vary [63,64], these components may dynamically cooperate to receive the different types of incoming SSs. An earlier study by Jan et al. [45] has shown that Sec66(Sec71)-dependent proteins contain an internal SS and enter the translocon as a looped conformation. Overexpression of Sec62, Sec63 or Sec72 in Sec71 deletion cells did not rescue translocation defects of Sec71-dependent proteins, suggesting that the function of Sec71 in efficient translocation initiation of internal hydrophobic SSs cannot be replaced by other subunits. Our study suggests that heterogeneous SSs encounter the Sec translocon differently and dynamically associate with Sec62, Sec63, Sec71 and Sec72 components for efficient translocation initiation *in vivo*.

Supplementary data to this article can be found online at https://doi.org/10.1016/j.bbamcr.2018.08.018.

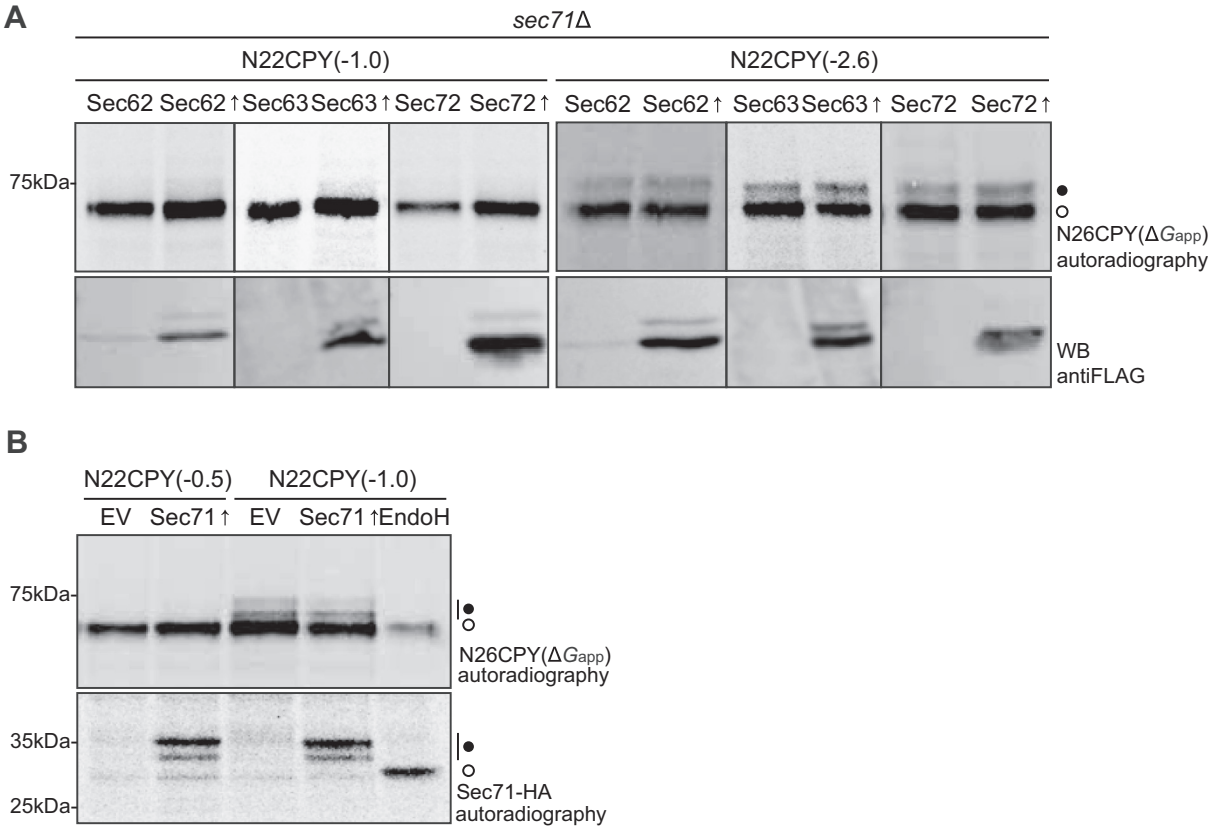

Fig. 4. Sec71 functions within a complex. (A) N22CPY(-1.0) or N22CPY(-2.6) were expressed in *sec71*Δ strain expressing FLAG tagged Sec62, 63 or 72 under endogenous or overexpression promoter. *Top*, proteins were analyzed as in Fig. 1B. *Bottom*, proteins were subjected to SDS-PAGE and detected by Western blotting using FLAG antibody. '↑' indicates overexpression. (B) N22CPY(-0.5) or N22CPY(-1.0) were expressed in genomically HA tagged *SEC71-HA* strain transformed with an empty vector (EV) or Sec71-HA overexpression vector (Sec71↑). N#CPY(ΔG_{app}) variants were analyzed as in Fig. 1B. N22CPY(-1.0) in Sec71-HA overexpression strain was treated with Endo H. Open and closed circles indicate glycosylated and non-glycosylated bands, respectively.

Conflict of interest

Authors declare no conflict of interest.

Transparency document

The Transparency document associated with this article can be found, in online version.

Acknowledgments

Authors thank the lab members for discussion and critical reading of the manuscript. This work was supported by grants from National Research Foundation of Korea (NRF-2016R1A2B2013459) and Promising-Pioneering Researcher Program through Seoul National University to HK.

Author contributions

JK, HK conceived the project, CY, SJ, JK, HK designed, analyzed data and wrote the manuscript. CY, SJ, JK, YJ, SJ conducted experiments.

References

[1] G. Blobel, B. Dobberstein, Transfer of proteins across membranes. I. Presence of proteolytically processed and unprocessed nascent immunoglobulin light chains on membrane-bound ribosomes of murine myeloma, J. Cell Biol. 67 (1975) 835–851.
[2] T.N. Petersen, S. Brunak, G. von Heijne, H. Nielsen, SignalP 4.0: discriminating signal peptides from transmembrane regions, Nat. Methods 8 (2011) 785–786.
[3] R.J. Keenan, D.M. Freymann, R.M. Stroud, P. Walter, The signal recognition particle, Annu. Rev. Biochem. 70 (2001) 755–775.
[4] M. Wiedmann, A. Huth, T.A. Rapoport, A signal sequence is required for the functions of the signal recognition particle, Biochem. Biophys. Res. Commun. 134 (1986) 790–796.
[5] T.V. Kurzchalia, M. Wiedmann, A.S. Girshovich, E.S. Bochkareva, H. Bielka, T.A. Rapoport, The signal sequence of nascent preprolactin interacts with the 54K polypeptide of the signal recognition particle, Nature 320 (1986) 634–636.
[6] T. Ast, G. Cohen, M. Schuldiner, A network of cytosolic factors targets SRP-independent proteins to the endoplasmic reticulum, Cell 152 (2013) 1134–1145.
[7] K. Plath, T.A. Rapoport, Spontaneous release of cytosolic proteins from post-translational substrates before their transport into the endoplasmic reticulum, J. Cell Biol. 151 (2000) 167–178.
[8] E.A. Costa, K. Subramanian, J. Nunnari, J.S. Weissman, Defining the physiological role of SRP in protein-targeting efficiency and specificity, Science 359 (2018) 689–692.
[9] R.M. Voorhees, R.S. Hegde, Structure of the Sec61 channel opened by a signal sequence, Science 351 (2016) 88–91.
[10] L. Li, E. Park, J. Ling, J. Ingram, H. Ploegh, T.A. Rapoport, Crystal structure of a substrate-engaged SecY protein-translocation channel, Nature 531 (2016) 395–399.
[11] R.A. Corey, W.J. Allen, J. Komar, S. Masiulis, S. Menzies, A. Robson, I. Collinson, Unlocking the bacterial SecY translocon, Structure 24 (2016) 518–527.
[12] E. Park, J.F. Menetret, J.C. Gumbart, S.J. Ludtke, W. Li, A. Whynot, T.A. Rapoport, C.W. Akey, Structure of the SecY channel during initiation of protein translocation, Nature 506 (2014) 102–106.
[13] Y. Ge, A. Draycheva, T. Bornemann, M.V. Rodnina, W. Wintermeyer, Lateral opening of the bacterial translocon on ribosome binding and signal peptide insertion, Nat. Commun. 5 (2014) 5263.
[14] P.F. Egea, R.M. Stroud, Lateral opening of a translocon upon entry of protein suggests the mechanism of insertion into membranes, Proc. Natl. Acad. Sci. U. S. A. 107 (2010) 17182–17187.
[15] K. Plath, B.M. Wilkinson, C.J. Stirling, T.A. Rapoport, Interactions between Sec complex and prepro-alpha-factor during posttranslational protein transport into the endoplasmic reticulum, Mol. Biol. Cell 15 (2004) 1–10.
[16] K. Plath, W. Mothes, B.M. Wilkinson, C.J. Stirling, T.A. Rapoport, Signal sequence recognition in posttranslational protein transport across the yeast ER membrane, Cell 94 (1998) 795–807.
[17] S.K. Lyman, R. Schekman, Binding of secretory precursor polypeptides to a

translocon subcomplex is regulated by BiP, Cell 88 (1997) 85–96.
[18] N. Aviram, T. Ast, E.A. Costa, E.C. Arakel, S.G. Chuartzman, C.H. Jan, S. Hassdenteufel, J. Dudek, M. Jung, S. Schorr, R. Zimmermann, B. Schwappach, J.S. Weissman, M. Schuldiner, The SND proteins constitute an alternative targeting route to the endoplasmic reticulum, Nature 540 (2016) 134–138.
[19] M. Schuldiner, J. Metz, V. Schmid, V. Denic, M. Rakwalska, H.D. Schmitt, B. Schwappach, J.S. Weissman, The GET complex mediates insertion of tail-anchored proteins into the ER membrane, Cell 134 (2008) 634–645.
[20] S. Stefanovic, R.S. Hegde, Identification of a targeting factor for posttranslational membrane protein insertion into the ER, Cell 128 (2007) 1147–1159.
[21] R.S. Hegde, H.D. Bernstein, The surprising complexity of signal sequences, Trends Biochem. Sci. 31 (2006) 563–571.
[22] B. Martoglio, B. Dobberstein, Signal sequences: more than just greasy peptides, Trends Cell Biol. 8 (1998) 410–415.
[23] G. von Heijne, Patterns of amino acids near signal-sequence cleavage sites, Eur. J. Biochem. 133 (1983) 17–21.
[24] L. Kocik, T. Junne, M. Spiess, Orientation of internal signal-anchor sequences at the Sec61 translocon, J. Mol. Biol. 424 (2012) 368–378.
[25] M. Higy, T. Junne, M. Spiess, Topogenesis of membrane proteins at the endoplasmic reticulum, Biochemistry 43 (2004) 12716–12722.
[26] V. Goder, M. Spiess, Molecular mechanism of signal sequence orientation in the endoplasmic reticulum, EMBO J. 22 (2003) 3645–3653.
[27] K. Rosch, D. Naeher, V. Laird, V. Goder, M. Spiess, The topogenic contribution of uncharged amino acids on signal sequence orientation in the endoplasmic reticulum, J. Biol. Chem. 275 (2000) 14916–14922.
[28] V. Goder, C. Bieri, M. Spiess, Glycosylation can influence topogenesis of membrane proteins and reveals dynamic reorientation of nascent polypeptides within the translocon, J. Cell Biol. 147 (1999) 257–266.
[29] J.M. Wahlberg, M. Spiess, Multiple determinants direct the orientation of signal-anchor proteins: the topogenic role of the hydrophobic signal domain, J. Cell Biol. 137 (1997) 555–562.
[30] M. Spiess, Heads or tails–what determines the orientation of proteins in the membrane, FEBS Lett. 369 (1995) 76–79.
[31] A.J. Denzer, C.E. Nabholz, M. Spiess, Transmembrane orientation of signal-anchor proteins is affected by the folding state but not the size of the N-terminal domain, EMBO J. 14 (1995) 6311–6317.
[32] M. Sakaguchi, R. Tomiyoshi, T. Kuroiwa, K. Mihara, T. Omura, Functions of signal and signal-anchor sequences are determined by the balance between the hydrophobic segment and the N-terminal charge, Proc. Natl. Acad. Sci. U. S. A. 89 (1992) 16–19.
[33] J.P. Beltzer, K. Fiedler, C. Fuhrer, I. Geffen, C. Handschin, H.P. Wessels, M. Spiess, Charged residues are major determinants of the transmembrane orientation of a signal-anchor sequence, J. Biol. Chem. 266 (1991) 973–978.
[34] E. Hartmann, T.A. Rapoport, H.F. Lodish, Predicting the orientation of eukaryotic membrane-spanning proteins, Proc. Natl. Acad. Sci. U. S. A. 86 (1989) 5786–5790.
[35] G. Heijne, The distribution of positively charged residues in bacterial inner membrane proteins correlates with the trans-membrane topology, EMBO J. 5 (1986) 3021–3027.
[36] Y. Harada, H. Li, J.S. Wall, H. Li, W.J. Lennarz, Structural studies and the assembly of the heptameric post-translational translocon complex, J. Biol. Chem. 286 (2011) 2956–2965.
[37] S. Panzner, L. Dreier, E. Hartmann, S. Kostka, T.A. Rapoport, Posttranslational protein transport in yeast reconstituted with a purified complex of Sec proteins and Kar2p, Cell 81 (1995) 561–570.
[38] R.J. Deshaies, S.L. Sanders, D.A. Feldheim, R. Schekman, Assembly of yeast Sec proteins involved in translocation into the endoplasmic reticulum into a membrane-bound multisubunit complex, Nature 349 (1991) 806–808.
[39] S.J. Jung, J.E. Kim, J.H. Reithinger, H. Kim, The Sec62-Sec63 translocon facilitates translocation of the C-terminus of membrane proteins, J. Cell Sci. 127 (2014) 4270–4278.
[40] J.H. Reithinger, J.E. Kim, H. Kim, Sec62 protein mediates membrane insertion and orientation of moderately hydrophobic signal anchor proteins in the endoplasmic reticulum (ER), J. Biol. Chem. 288 (2013) 18058–18067.
[41] A. Mades, K. Gotthardt, K. Awe, J. Stieler, T. Doring, S. Fuser, R. Prange, Role of human sec63 in modulating the steady-state levels of multi-spanning membrane proteins, PLoS One 7 (2012) e49243.
[42] B.P. Young, R.A. Craven, P.J. Reid, M. Willer, C.J. Stirling, Sec63p and Kar2p are required for the translocation of SRP-dependent precursors into the yeast endoplasmic reticulum in vivo, EMBO J. 20 (2001) 262–271.
[43] J.L. Brodsky, J. Goeckeler, R. Schekman, BiP and Sec63p are required for both co- and posttranslational protein translocation into the yeast endoplasmic reticulum, Proc. Natl. Acad. Sci. U. S. A. 92 (1995) 9643–9646.
[44] H.A. Meyer, H. Grau, R. Kraft, S. Kostka, S. Prehn, K.U. Kalies, E. Hartmann, Mammalian Sec61 is associated with Sec62 and Sec63, J. Biol. Chem. 275 (2000) 14550–14557.
[45] C.H. Jan, C.C. Williams, J.S. Weissman, Principles of ER cotranslational translocation revealed by proximity-specific ribosome profiling, Science 346 (2014) 1257521.
[46] B.M. Wilkinson, J.R. Tyson, C.J. Stirling, Ssh1p determines the translocation and dislocation capacities of the yeast endoplasmic reticulum, Dev. Cell 1 (2001) 401–409.
[47] K. Kitada, E. Yamaguchi, M. Arisawa, Cloning of the *Candida glabrata* TRP1 and HIS3 genes, and construction of their disruptant strains by sequential integrative transformation, Gene 165 (1995) 203–206.
[48] K.R. Oldenburg, K.T. Vo, S. Michaelis, C. Paddon, Recombination-mediated PCR-directed plasmid construction in vivo in yeast, Nucleic Acids Res. 25 (1997) 451–452.
[49] T. Hessa, N.M. Meindl-Beinker, A. Bernsel, H. Kim, Y. Sato, M. Lerch-Bader, I. Nilsson, S.H. White, G. von Heijne, Molecular code for transmembrane-helix recognition by the Sec61 translocon, Nature 450 (2007) 1026–1030.
[50] H. Kim, K. Melen, M. Osterberg, G. von Heijne, A global topology map of the *Saccharomyces cerevisiae* membrane proteome, Proc. Natl. Acad. Sci. U. S. A. 103 (2006) 11142–11147.
[51] S.F. Trueman, E.C. Mandon, R. Gilmore, A gating motif in the translocation channel sets the hydrophobicity threshold for signal sequence function, J. Cell Biol. 199 (2012) 907–918.
[52] T. Junne, T. Schwede, V. Goder, M. Spiess, Mutations in the Sec61p channel affecting signal sequence recognition and membrane protein topology, J. Biol. Chem. 282 (2007) 33201–33209.
[53] D.T. Ng, J.D. Brown, P. Walter, Signal sequences specify the targeting route to the endoplasmic reticulum membrane, J. Cell Biol. 134 (1996) 269–278.
[54] I. Nilsson, P. Whitley, G. von Heijne, The COOH-terminal ends of internal signal and signal-anchor sequences are positioned differently in the ER translocase, J. Cell Biol. 126 (1994) 1127–1132.
[55] S.U. Heinrich, T.A. Rapoport, Cooperation of transmembrane segments during the integration of a double-spanning protein into the ER membrane, EMBO J. 22 (2003) 3654–3663.
[56] M. Hermansson, G. von Heijne, Inter-helical hydrogen bond formation during membrane protein integration into the ER membrane, J. Mol. Biol. 334 (2003) 803–809.
[57] S.K. Lyman, R. Schekman, Interaction between BiP and Sec63p is required for the completion of protein translocation into the ER of *Saccharomyces cerevisiae*, J. Cell Biol. 131 (1995) 1163–1171.
[58] A.K. Corsi, R. Schekman, The lumenal domain of Sec63p stimulates the ATPase activity of BiP and mediates BiP recruitment to the translocon in Saccharomyces cerevisiae, J. Cell Biol. 137 (1997) 1483–1493.
[59] B. Jadhav, M. McKenna, N. Johnson, S. High, I. Sinning, M.R. Pool, Mammalian SRP receptor switches the Sec61 translocase from Sec62 to SRP-dependent translocation, Nat. Commun. 6 (2015) 10133.
[60] A. Guna, R.S. Hegde, Transmembrane domain recognition during membrane protein biogenesis and quality control, Curr. Biol. 28 (2018) R498–R511.
[61] T. Kriegler, A. Magoulopoulou, R. Amate Marchal, T. Hessa, Measuring endoplasmic reticulum signal sequences translocation efficiency using the Xbp1 arrest peptide, Cell Chem. Biol. 25 (2018) 880–890.
[62] S. Hassdenteufel, N. Johnson, A.W. Paton, J.C. Paton, S. High, R. Zimmermann, Chaperone-mediated Sec61 channel gating during ER import of small precursor proteins overcomes Sec61 inhibitor-reinforced energy barrier, Cell Rep. 23 (2018) 1373–1386.
[63] N.A. Kulak, G. Pichler, I. Paron, N. Nagaraj, M. Mann, Minimal, encapsulated proteomic-sample processing applied to copy-number estimation in eukaryotic cells, Nat. Methods 11 (2014) 319–324.
[64] S. Ghaemmaghami, W.K. Huh, K. Bower, R.W. Howson, A. Belle, N. Dephoure, E.K. O'Shea, J.S. Weissman, Global analysis of protein expression in yeast, Nature 425 (2003) 737–741.

Abbreviations

ER: endoplasmic reticulum
SS: signal sequence
SRP: signal recognition particle
SP: signal peptide
SA: signal anchor
CPY: carboxypeptidase Y
TMD: transmembrane domain
Endo H: endoglycosidase H